Structural basis of pH-dependent activation in a CLC transporter

In the format provided by the
authors and unedited

Supplementary Information for

Structural basis of pH-dependent activation in a CLC transporter

Eva Fortea[#], Sangyun Lee[#], Rahul Chadda, Yiorgos Argyros, Priyanka Sandal, Robyn Mahoney-Kruszka, Didar Ciftici, Maria E. Falzone, Gerard Huysmans, Janice L. Robertson, Olga Boudker[*] and Alessio Accardi[*]

* Correspondence to:

Alessio Accardi: ala2022@med.cornell.edu

Olga Boudker: olb2003@med.cornell.edu

# These authors contributed equally to the work
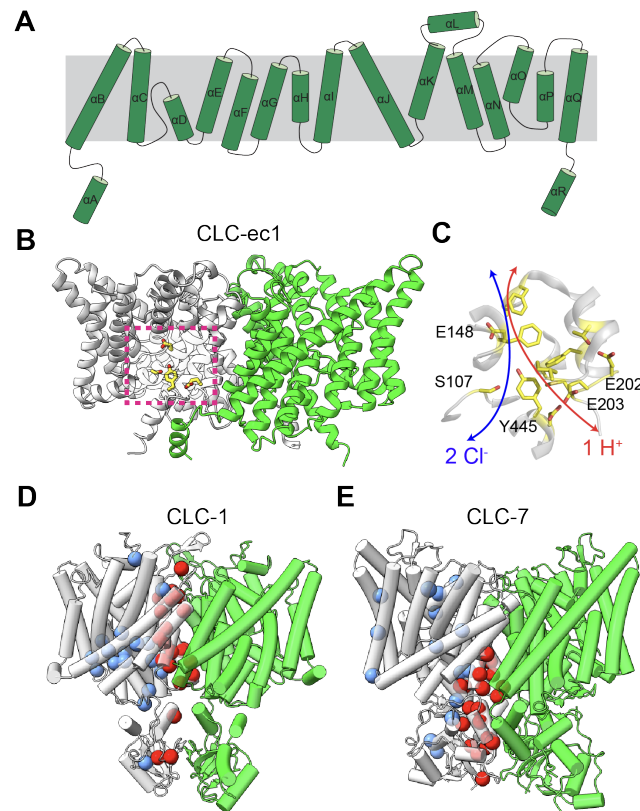
Supplementary Figure 1: CLC structural organization. (A) CLC-ec1 transmembrane topology. The residue numbers are shown at the N and C termini of helices A-R. **(B)** Side view of the structure of CLC-ec1 dimer (PDB: 1OTS). The cartoon representation of each protomer is colored in light gray and green. The sidechain of important residues (S107, E148, E203, and Y445) are shown in stick models and colored yellow in protomer A. The region where the Cl⁻ and H⁺ pathways cross is highlighted by a dashed pink box. **(C)** Close-up view of the highlighted region. The side chains of residues lining the Cl⁻ pore (delineated by a blue arrow) and the H⁺ pathway (delineated by a red arrow) are shown as sticks. S107 and Y445 delimit the intracellular constriction, and E148 occludes the extracellular constriction in the Cl⁻ pore. E202 and E203 define the intracellular vestibule of the H⁺ pathway. Also shown but not labeled are the following residues lining the H⁺ pathway: E113, A182, L186, A189, F190, F199, M204, F357, I402, and T407. **(E)** Locations of mutations causing dominant myotonia congenita [1-4] are mapped onto the protomer A of CLC-1 (PDB: 6QVC)[5]. **(D)** Mutations causing dominant osteopetrosis [6] are mapped onto protomer A of CLC-7 (PDB: 7JMJ)[7]. Mutations within 12 Å of the sister protomer are shown as red spheres (21 out of 38 for CLC-1 and 21 out of 35 for CLC-7), and mutations further away are shown as light blue spheres.
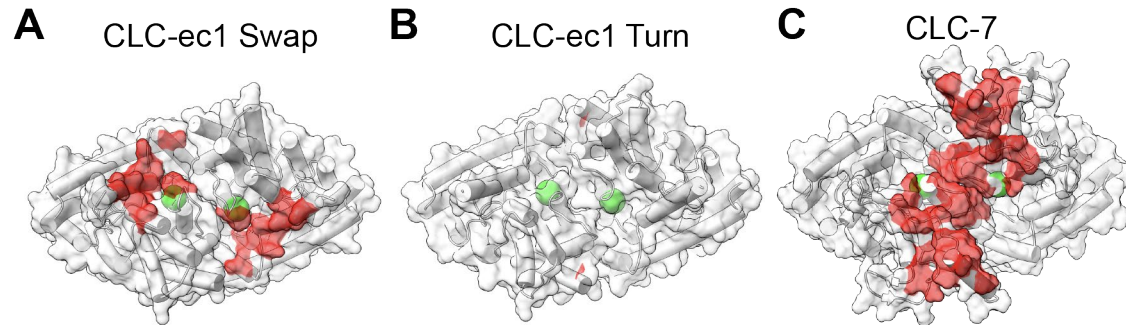
Supplementary Figure 2. Transmembrane-cytosolic interface in CLC channels and transporters. (A-C) The transmembrane (TM) domain of CLC-ec1 in Swap **(A)**, Turn (B), CLC-7 (PDB:7JM7) **(C)** is viewed from the intracellular side. The TM domain is shown in gray surface and cartoon, the cytosolic domain is not shown. For CLC-ec1, the cytosolic domain is the N-terminal αA helix. In all panels, the interface between the TM and cytosolic domains is colored in red. A residue is defined as part of the interface when its Cα-Cα distance from any residues in the cytosolic domain is < 8 Å. E203 of CLC-ec1 and E314 of CLC-7, which indicate the entrance of the intracellular vestibule of the H$^+$ pathway, are shown as green spheres.

System	CLC-ec1	pH	Initial Velocity (μM Cl$^-$ s^{-1} ± SD)	n
1	CLC-ec1	4.5	4.52 ± 0.24	9
2	CLC-ec1*	4.5	4.22 ± 0.11	9
	CLC-ec1	7.5	0.24 ± 0.09	5
3	L25C/A450C	4.5	1.13 ± 0.06	9
4	L25C/A450C*	4.5	2.44 ± 0.09	9
5	L25C	4.5	3.37 ± 0.20	9
6	L25C*	4.5	3.62 ± 0.22	9
7	A450C	4.5	3.43 ± 0.14	9
8	A450C*	4.5	3.52 ± 0.15	9
9	R230C/L249C^	4.5	3.55 ± 0.23	3
10	R230C/L249C*^	4.5	3.51 ± 0.33	2
11	L25C/A450C/ R230C/L249C	4.5	1.30 ± 0.12	9
12	L25C/A450C/ R230C/L249C*	4.5	2.79 ± 0.13	9
13	E385C^	4.5	2.95 ± 0.85	6
14	Q24C	4.5	2.14 ± 0.54	10
15	Q24C-labelled	4.5	3.84 ± 0.09	9
16	Q24C	7.5	0.24 ± 0.08	9
17	Q24C E202Q	4.5	0.47 ± 0.12	9
18	Q24C E202Q	7.5	0.14 ± 0.05	11
19	Q24C E202Y^	4.5	0.13 ± 0.05	5
20	Q24C I201W	4.5	0.78 ± 0.22	9
21	Q24C I201W	7.5	0.17 ± 0.07	10

Supplementary Table 1: Cl$^-$ transport rates of CLC-ec1 constructs. Initial velocity of Cl$^-$ efflux from proteoliposomes reconstituted with WT or mutant CLC-ec1 reconstituted at 0.2 μg protein/mg of lipid. Initial velocity was measured with a linear fit of the initial portion of the flux time course and is reported in μM Cl$^-$ s^{-1} ± SD of 5+ independent experiments from 3 independent reconstitutions unless otherwise stated. * denotes liposomes treated with 30 mM TCEP for 1 hr after extrusion prior to functional measurements. ^ denotes previously characterized CLC-ec1 mutations and therefore these constructs were tested in N=1 (R230C/L249C) [8] or N=2 (E385C) [9] independent preparations. Q24C-labelled was generated by incubating Q24C with maleimide activated LD555p and LD650 fluorophores in the same molar ratio used in smFRET TIRF imaging (CLC-ec1:LD555p:LD650 = 1:2:2.5). The labelled E385C mutant was shown to be as active as the unlabeled form in previous work [10].

	pH	Cl⁻ (mM)	E385C					Q24C				
			Full interface		Reduced interface		N	Helix A bound		Helix A loose		N
			(mean ± SD)	%	(mean ± SD)	%		(mean ± SD)	%	(mean ± SD)	%	
WT	7.5	0	0.83 ± 0.06	100	-	-	754	0.85 ± 0.08	62	0.46 ± 0.09	38	962
WT	7.5	100	0.84 ± 0.06	90	0.42 ± 0.10	10	1167	0.85 ± 0.07	67	0.46 ± 0.07	33	1145
WT	4.5	0	0.80 ± 0.06	88	0.57 ± 0.15	12	924	0.72 ± 0.10	16	0.56 ± 0.07	84	1238
WT	4.5	100	0.79 ± 0.06	64	0.44 ± 0.18	36	1113	0.78 ± 0.07	26	0.54 ± 0.08	74	1719
E202Q	7.5	100	0.84 ± 0.07	100	-	-	1003	0.77 ± 0.06	12	0.46 ± 0.08	88	753
E202Q	4.5	100	0.78 ± 0.07	45	0.26 ± 0.10 / 0.53 ± 0.10	55	942	0.77 ± 0.10	17	0.56 ± 0.10	83	975
E202Y	7.5	100	0.82 ± 0.07	100	-	-	1172	-	-	0.46 ± 0.08	100	1145
E202Y	4.5	100	0.78 ± 0.08	100	-	-	848	-	-	0.54 ± 0.09	100	920
I201W	7.5	100	0.79 ± 0.08	88	0.45 ± 0.20	12	871	0.85 ± 0.06	100	-	-	1099
I201W	4.5	100	0.76 ± 0.07	40	0.41 ± 0.18	60	696	0.80 ± 0.40	20	0.66 ± 0.13 / 0.20 ± 0.07	80	1201

Supplementary Table 2: smFRET summary table. Populations obtained from Gaussian fitting of time averaged distributions at pH 4.5 or 7.5 in the presence or absence of chloride. Data shown is the mean ± SD of 3+ independent reconstitutions. N is the total number of molecules.

System Number	Starting conformation	Protonation of E202	Cut-off pKa	Cl$^-$ in S$_{cen}$
1	Swap	E202(0)	pH 4.5	Yes
2	Swap	E202(0)	pH 7.5	Yes
3	Turn	E202(0)	pH 4.5	Yes
4	Twist	E202(0)	pH 4.5	Yes
5	Bot-Inter	E202(0)	pH 4.5	Yes
6	E202Y	N/A	pH 4.5	Yes
7	Swap	E202(0)	pH 4.5	No
8	Swap	E202(-)*	pH 4.5	No

Supplementary Table 3: Systems used for free MD simulations. List of protonation states and Cl$^-$ occupancy of the central binding site. E202(0) and E202(-) denote a protonated and deprotonated E202 side chain, respectively. * denotes that E202 was set to be deprotonated at pH 4.5 where it would normally be protonated. The protonation state of other residues was determined using cut-off pKa value of 4.5 and 7.5 to mimic experimental conditions (see Methods and Fig. 4 Supp. 1A). Ten independent replicas of 1 µs long trajectory (10 µs in total) were generated for each system.

CLC-ec1	hCLC-1	hCLC-3	hCLC-4	hCLC-5	hCLC-7
I201	I290M[11,12]		L279V[13]		
E202	E291K[14]		E280D[13]	E337(E267)A[15], K[16], V[17], or del[18]	E313 (E289)K[19,20]
I422	I556N[21]	I607T[22]	I549T[13]		

Supplementary Table 4. Disease-causing mutations in human CLCs at positions corresponding to I201, E202, and I422 in CLC-ec1. The numbers in the parenthesis denote the amino acid sequence number from different isoforms. "del" denotes a deletion mutant.

System No.	Initial position of αA	Protonation of E202	Cut-off pKa
12, forward	Bound	E202(0)	pH 4.5
12, reverse	Loose	E202(0)	pH 4.5
13, forward	Bound	E202(0)	pH 7.5
13, reverse	Loose	E202(0)	pH 7.5
14, forward	Bound	E202(-)	pH 4.5
14, reverse	Loose	E202(-)	pH 4.5
15, forward	Bound	E202(-)	pH 7.5
15, reverse	Loose	E202(-)	pH 7.5

Supplementary Table 5: Molecular systems used for PMF calculations. The starting conformation of the TM region of CLC-ec1 was the Swap cryoEM conformation determined at pH 4.5 and 100 mM Cl^-. αA bound indicates a conformation where it interacts with αR of the opposite subunit. αA loose refers to a conformation where it rotates away from the transmembrane region of the exchanger and is ~ parallel to the plane of the membrane, as seen in Turn and Twist cryoEM conformations as well as in free MD simulations. In all cases no Cl^- was placed in S_{cen}. E202(0) and E202(-) denote a protonated and deprotonated E202 side chain, respectively. The protonation state of other residues was determined using a cut-off pKa value of 4.5 and 7.5 to mimic experimental conditions (see Methods and Fig. 4 Supp. 1A). Each calculation was performed using 105 windows of 30 ns each for sampling.

ClC-7[PM]	Current density at +80 mV (pA/pF) ± SEM	τ at +80 mV (ms) ± SEM	n
WT	20.3 ± 3.1	962 ± 69	9
E311Q	15.9 ± 1.8	192 ± 15	9
L310W	45.2 ± 5.8	38 ± 4	9
G578W	27.7 ± 4.3	37 ± 4	10
L310W+G578W	21.4 ± 3.0	36 ± 5	9

Supplementary Table 6: Electrophysiological characterization of WT and mutant CLC-7[PM] constructs. Current density and activation time constant, τ, at +80 mV of WT and mutant CLC-7PM expressed in HEK293 cells were determined using whole cell patch clamp electrophysiology. τ was determined from a single exponential fit of the currents. Data is reported as mean ± SEM of n cells from 3+ independent transfections.

Structure	PDB	EMDB
CLC-ec1 pH 7.5 0 mM Cl⁻ Swap	7RNX	EMD-24582
CLC-ec1pH 7.5 100 mM Cl⁻ Swap	7RO0	EMD-24584
CLC-ec1pH 4.5 0 mM Cl⁻ Swap	7RP6	EMD-24668
CLC-ec1pH 4.5 0 mM Cl⁻ Turn	7RSB	EMD-24583
CLC-ec1pH 4.5 100 mM Cl⁻ Swap	7N8P	EMD-24241
CLC-ec1pH 4.5 100 mM Cl⁻ Turn	7RP5	EMD-24612
CLC-ec1pH 4.5 100 mM Cl⁻ Twist	7N0W	EMD-24263
R230C/L249C pH 4.5 100mM Cl⁻ Swap	8GA1	EMD-29884
R230C/L249C pH 4.5 100mM Cl⁻ Turn	8GA3	EMD-29885
L25C/A450C pH 4.5 100mM Cl⁻ Intermediate	8GA5	EMD-29890
L25C/A450C pH 4.5 100mM Cl⁻ Twist	8GAH	EMD-29899
E202Y pH 4.5 100mM Cl⁻	8GA0	EMD-29883

Supplementary Table 7: Accession Codes

Structure	PDB	EMDB
CLC-ec1 pH 7.5 0 mM Cl⁻ Swap	7RNX	EMD-24582
CLC-ec1pH 7.5 100 mM Cl⁻ Swap	7RO0	EMD-24584
CLC-ec1pH 4.5 0 mM Cl⁻ Swap	7RP6	EMD-24668
CLC-ec1pH 4.5 0 mM Cl⁻ Turn	7RSB	EMD-24583
CLC-ec1pH 4.5 100 mM Cl⁻ Swap	7N8P	EMD-24241
CLC-ec1pH 4.5 100 mM Cl⁻ Turn	7RP5	EMD-24612
CLC-ec1pH 4.5 100 mM Cl⁻ Twist	7N9W	EMD-24263
R230C/L249C pH 4.5 100mM Cl⁻ Swap	8GA1	EMD-29884
R230C/L249C pH 4.5 100mM Cl⁻ Turn	8GA3	EMD-29885
L25C/A450C pH 4.5 100mM Cl⁻ Intermediate	8GA5	EMD-29890
L25C/A450C pH 4.5 100mM Cl⁻ Twist	8GAH	EMD-29899
E202Y pH 4.5 100mM Cl⁻	8GA0	EMD-29883

Supplementary Table 7: Accession Codes

References

1 Suetterlin, K. *et al.* Translating genetic and functional data into clinical practice: a series of 223 families with myotonia. *Brain : a journal of neurology* **145**, 607-620 (2022). https://doi.org/10.1093/brain/awab344

2 Pusch, M. Myotonia caused by mutations in the muscle chloride channel gene CLCN1. *Hum. Mutat.* **19**, 423-434 (2002).

3 Dupré, N. *et al.* Clinical, electrophysiologic, and genetic study of non-dystrophic myotonia in French-Canadians. *Neuromuscular disorders : NMD* **19**, 330-334 (2009). https://doi.org/10.1016/j.nmd.2008.01.007

4 Altamura, C. *et al.* The analysis of myotonia congenita mutations discloses functional clusters of amino acids within the CBS2 domain and the C-terminal peptide of the ClC-1 channel. *Hum Mutat* **39**, 1273-1283 (2018). https://doi.org/10.1002/humu.23581

5 Wang, K. *et al.* Structure of the human ClC-1 chloride channel. *PLOS Biology* **17**, e3000218 (2019). https://doi.org/10.1371/journal.pbio.3000218

6 Zifarelli, G. The Role of the Lysosomal Cl(-)/H(+) Antiporter ClC-7 in Osteopetrosis and Neurodegeneration. *Cells* **11** (2022). https://doi.org/10.3390/cells11030366

7 Schrecker, M., Korobenko, J. & Hite, R. K. Cryo-EM structure of the lysosomal chloride-proton exchanger CLC-7 in complex with OSTM1. *eLife* **9**, e59555 (2020). https://doi.org/10.7554/eLife.59555

8 Nguitragool, W. & Miller, C. CLC Cl$^-$/H$^+$ transporters constrained by covalent cross-linking. *Proc. Natl. Acad. Sci. U. S. A.* **104**, 20659-20665 (2007).

9 Khantwal, C. M. *et al.* Revealing an outward-facing open conformational state in a CLC Cl(-)/H(+) exchange transporter. *Elife* **5** (2016). https://doi.org/10.7554/eLife.11189

10 Chavan, T. S. *et al.* A CLC-ec1 mutant reveals global conformational change and suggests a unifying mechanism for the CLC Cl$^-$/H$^+$ transport cycle. *eLife* **9**, e53479 (2020). https://doi.org/10.7554/eLife.53479

11 Koty, P. P., Pegoraro, E. & Hoffman, E. P. Linkage and mutation analysis of Thomsen and Becker myotonia families. *American Journal of Human Genetics* **55**, Medium: X; Size: pp. A227.1323 (1994).

12 Lehmann-Horn, F., Mailänder, V., Heine, R. & George, A. L. Myotonia levior is a chloride channel disorder. *Human Molecular Genetics* **4**, 1397-1402 (1995). https://doi.org/10.1093/hmg/4.8.1397

13 Palmer, E. E. *et al.* Functional and clinical studies reveal pathophysiological complexity of CLCN4-related neurodevelopmental condition. *Molecular Psychiatry* **28**, 668-697 (2023). https://doi.org/10.1038/s41380-022-01852-9

14 Meyer-Kleine, C., Steinmeyer, K., Ricker, K., Jentsch, T. J. & Koch, M. C. Spectrum of mutations in the major human skeletal muscle chloride channel gene (CLCN1) leading to myotonia. *Am J Hum Genet* **57**, 1325-1334 (1995).

15 Hoopes, R. R., Jr. *et al.* Evidence for genetic heterogeneity in Dent's disease. *Kidney Int* **65**, 1615-1620 (2004). https://doi.org/10.1111/j.1523-1755.2004.00571.x

16 Halbritter, J. *et al.* Fourteen Monogenic Genes Account for 15% of Nephrolithiasis/Nephrocalcinosis. *Journal of the American Society of Nephrology* **26**, 543-551 (2015). https://doi.org/10.1681/asn.2014040388

17 Minamikawa, S. *et al.* Development of ultra-deep targeted RNA sequencing for analyzing X-chromosome inactivation in female Dent disease. *Journal of Human Genetics* **63**, 589-595 (2018). https://doi.org/10.1038/s10038-018-0415-1

18   Tosetto, E. *et al.* Phenotypic and genetic heterogeneity in Dent's disease--the results of an Italian collaborative study. *Nephrol Dial Transplant* **21**, 2452-2463 (2006). https://doi.org/10.1093/ndt/gfl274

19   Wang, C. *et al.* The virulence gene and clinical phenotypes of osteopetrosis in the Chinese population: six novel mutations of the CLCN7 gene in twelve osteopetrosis families. *Journal of bone and mineral metabolism* **30**, 338-348 (2012). https://doi.org/10.1007/s00774-011-0319-z

20   Li, L., Lv, S.-S., Wang, C., Yue, H. & Zhang, Z.-L. Novel CLCN7 mutations cause autosomal dominant osteopetrosis type II and intermediate autosomal recessive osteopetrosis. *Mol Med Rep* **19**, 5030-5038 (2019). https://doi.org/10.3892/mmr.2019.10123

21   Plassart-Schiess, E. *et al.* Novel muscle chloride channel (CLCN1) mutations in myotonia congenita with various modes of inheritance including incomplete dominance and penetrance. *Neurology* **50**, 1176-1179 (1998).

22   Duncan, A. R. *et al.* Unique variants in CLCN3, encoding an endosomal anion/proton exchanger, underlie a spectrum of neurodevelopmental disorders. *The American Journal of Human Genetics* **108**, 1450-1465 (2021). https://doi.org/https://doi.org/10.1016/j.ajhg.2021.06.003